Applied Catalysis B: Environmental 178 (2015) 44–53

Contents lists available at ScienceDirect

Applied Catalysis B: Environmental

journal homepage: www.elsevier.com/locate/apcatb

Determination of main species involved in the first steps of TiO_2 photocatalytic degradation of organics with the use of scavengers: The case of ofloxacin

Eva M. Rodríguez*, Gracia Márquez, Miriam Tena, Pedro M. Álvarez, Fernando J. Beltrán

Departamento de Ingeniería Química y Química Física, Universidad de Extremadura, 06006 Badajoz, Spain

ARTICLE INFO

Article history:
Received 13 July 2014
Received in revised form 31 October 2014
Accepted 1 November 2014
Available online 13 November 2014

Keywords:
Ofloxacin
TiO_2 photocatalytic process
ROS
Scavengers
Phosphate

ABSTRACT

With the aid of different scavengers species involved in the first steps of TiO_2/UVA (black light) photocatalytic elimination of ofloxacin (OFX) in water have been investigated. The effect of the presence of scavengers of hydroxyl radicals in bulk water (*t*-butanol), oxidant holes (h^+) (2-propanol, iodide and oxalate), singlet oxygen (azide), electrons (oxygen) and superoxide ion radical (*p*-benzoquinone and tiron) has been checked at pH 7 with 0.03 M $HClO_4/ClO_4^-$ aerated media. The main elimination pathway leads to the formation of $OFX^{\bullet+}$ and takes place through an electronic transfer between the antibiotic and the catalyst surface. $OFX^{\bullet+}$ further reacts with $O_2^{\bullet-}$ leading to the reductive demethylation of OFX and generates 1 mole of hydrogen peroxide and ~1 mole of formaldehyde per mole of OFX eliminated. The presence of phosphate promotes a change in the pathway degradation, possibly favoring the generation of HO radicals as well as the participation of this species on the oxidative demethylation of OFX and therefore reduces the production of H_2O_2. Therefore, OFX can be photocatalytically reduced and/or oxidized depending on the experimental conditions.

1. Introduction

It is well known that advanced oxidation processes, AOPs, are appropriate technologies to remove emergent contaminants (ECs) from water [1]. These compounds, for which the risk to human health is not yet known, have been detected in global drinking water supplies at trace levels and are resistant to classical technologies applied in municipal wastewater treatment plants. Among AOPs photocatalytic treatment using UVA or solar light are of high interest for economic reasons. In most of cases, the mechanism of EC removal is via hydroxyl radical oxidation, especially when the radiation wavelength applied is higher than 350 nm and the direct photolysis of the EC is negligible [2,3]. In some cases, however, the mechanism of contaminant removal is not clear and other routes (photosensitizing, singlet oxygen action, direct oxidation by positive holes formed at the semiconductor valence band, etc.) are responsible of EC elimination [4]. In the light of the above, for this type of processes it is important to know the true pathway of removal in order to power the appropriate experimental conditions and therefore to increase the reaction rate.

In a previous paper we studied the photocatalytic TiO_2 P25/UVA (black light) degradation of a mixture of four EC (atenolol, hydrochlorotiazide, trimethoprim and ofloxacin) [4]. The results showed that while the first three indicated compounds (see their molecular structures in Fig. S1, supporting information) were mainly removed through their oxidation by the hydroxyl radicals formed in the bulk water, ofloxacin (OFX; see molecular structure in Fig. 1a) removal followed a different route. Moreover, the presence of OFX in solution seemed to inhibit the photocatalytic production of HO• radicals and hence the degradation of the other three EC. In this work, attention has been focused on the mechanism of TiO_2 photocatalytic removal of OFX using different substances recognized as scavengers of hydroxyl and/or superoxide ion radicals, positive holes, electrons, singlet oxygen, etc. Another objective was to discern whether or not these substances are appropriate for determining the species involved in the photocatalytic degradation of organics in water.

2. Experimental

Reagent grade ofloxacin, oxalic acid, sodium azide, *p*-benzoquinone, tiron (4,5-dihydroxy-1,3-benzenedisulfonic disodium salt) and *t*-butanol were obtained from Sigma–Aldrich, *p*-benzoquinone and hydrogen peroxide from Merck and 2-propanol

* Corresponding author. Tel.: +34 924 289 387; fax: +34 924 289 385.
E-mail address: evarguez@unex.es (E.M. Rodríguez).

http://dx.doi.org/10.1016/j.apcatb.2014.11.002
0926-3373/

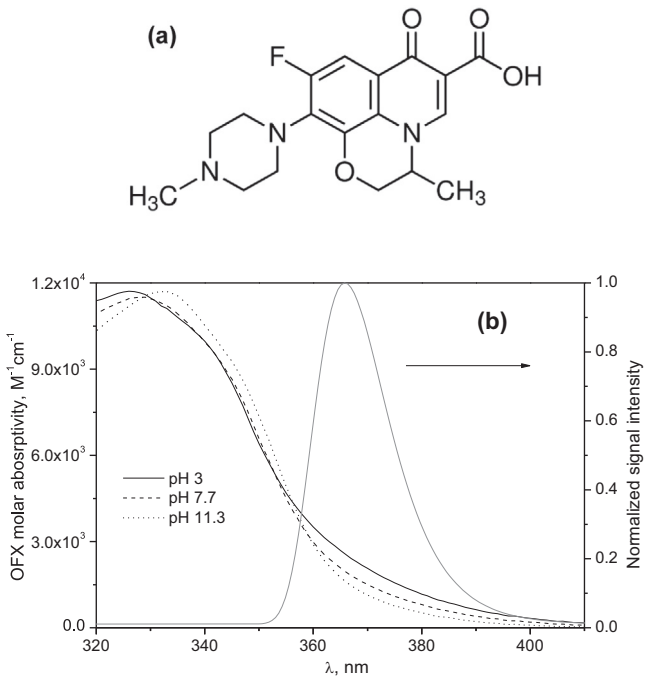

Fig. 1. (a) Structure of OFX. (b) Molar absorptivity of OFX as a function of pH and typical emission spectra of a black light blue lamp.

and potassium iodide from Panreac. The catalyst used was Aeroxide® TiO_2 P25 directly supplied by the manufacturer (Evonik Industries AG, Germany) and used as received. It is mainly composed of anatase and rutile crystallites (5.3 ± 0.28 anatase to rutile ratio) with a low content of amorphous phase [5]. It has a BET specific surface area of about 50 $m^2\ g^{-1}$ and primary particles of about 21 nm that form aggregates of several hundred nanometers [6].

All experiments were carried out in a 4 L borosilicate cylindrical reactor equipped with bubbling (air or nitrogen was fed through a porous plate situated at the reactor bottom), magnetic agitation and devices for measuring temperature and pH. The reactor was situated in the center of a 50 cm × 30 cm × 30 cm black wooden box where 2 15 W black light lamps (Lamp15TBL HQPower™ Velleman®) were placed in two opposing corners inside the box. These lamps emit radiation in the range 350–400 nm centered at ~370 nm. Parker reagent [7] that is, ferrioxalate, was used as actinometer to determine the incident photon flux, I_0, in the photoreactor, that was found to be 7.33×10^{-7} einstein s^{-1}.

The experimental procedure was started by turning on the lamps and waiting 30 min to reach their emission stationary state. Meanwhile, the reactor outside the wooden box was charged with an aqueous solution containing the pharmaceutical compound (at concentrations of 7.5 or 15 μM) and an appropriate amount of the scavenger (when needed). The solution pH was then adjusted to 7 with perchloric acid and sodium hydroxide (final perchloric/perchlorate concentration 0.03 M). In most cases pH changed no more than 0.5 units during the reaction time (2 h). When pH decreased below 6.5 some drops of concentrated NaOH were added. Finally, in photocatalytic experiments 0.1 g L^{-1} of TiO_2 was immediately added just after the experiment start up. In most of the runs air was continuously bubbled through the aqueous solution at a flow rate of 30 L h^{-1} but in a few cases, nitrogen was used instead or the experiment was carried out without gas feeding. Also, in some experiments no black light or TiO_2 were applied to study the adsorption of OFX on TiO_2 or its direct photolysis, respectively. In all runs, at regular intervals, samples were withdrawn from the reactor and filtered (PET Macherey-Nagel, 0.20 μm) before their analysis.

Concentrations of OFX, TOC, hydrogen peroxide, formaldehyde and Total Antioxidant Capacity (TAC) were measured. For OFX and TOC analysis a few microliters of 1 M sodium thiosulfate were added to aliquots of the samples to avoid the progress of any possible oxidation reaction. Concentration of OFX was determined by HPLC-DAD (Elite La Chrom) with a 5 μm 15 cm × 0.3 cm Phenomenex Gemini C18 column eluting the compound in isocratic form. The mobile phase was a mixture of 15/85 acetonitrile/water (acidified with phosphoric acid 1%, v/v), pumped at a flow rate of 0.5 mL min^{-1}. Detection was made with a L-2455 Hitachi diode array detector at 290 nm and the retention time was 6 min. Total organic carbon was monitored with a TOC-V_{SCH} Shimadzu carbon analyzer. Hydrogen peroxide was determined with the method of Masschelein et al. [8]. Also, any possible reaction of the different scavengers with H_2O_2 as well as their possible interference on Masschelein's method were checked. The concentration of formaldehyde in solution was determined by the Hantzsch reaction measuring the absorbance at 412 nm of the diacetyldihydrolutidine formed ($\varepsilon_{412\,nm}$ = 7530 $M^{-1}\ cm^{-1}$, [9]) using a 50 mm optical pathlength glass cell. TAC (related to the presence of reducing agents) was determined using the Folin-Ciocalteau method, an electron transfer based TAC assay [10,11]. TAC was expressed as equivalents of OFX, compound that gives a high response to the Folin-Ciocalteau analysis [4,12]. The TAC corresponding to the intermediates formed (TAC-I) was calculated by substracting OFX concentration (measured by HPLC-DAD) to TAC.

The first intermediates generated during the photocatalytic degradation of OFX were determined by liquid chromatography–electrospray ionization-quadrupole-time-of-flight-mass spectrometry (LC–ESI-QTOFMS) working in positive ionization mode. The compounds were separated using a HPLC system (Agilent 1260 Series) equipped with a Kromasil 100-5 C18 analytical column of 15 cm × 0.4 cm. Isocratic elution was performed with 15/85 ACN/H_2O (Milli Q) 0.1% formic acid at a flow rate of 1 mL min^{-1}. The volume of injection was 5 μL. The HPLC system was connected to a QTOF mass spectrometer (Agilent 6530 Series). The instrument was operated in the 4 GHz high-resolution mode. Ions were generated using an electrospray ion source dual ESI. Electrospray conditions were as follows: capillary, 3500 V; nebulizer, 30 psi; drying gas, 60 L/min; gas temperature, 350 °C; skimmer voltage, 65 V; octapoleRFPeak, 750 V; fragmentor, 200 V. The mass axis was calibrated using the mixture provided by the manufacturer over the m/z 70–1000 range. A sprayer with a reference solution was used as continuous calibration in positive ion using the following reference masses: 121.0509 and 922.0098 m/z. Data were processed with the Agilent MassHunter Workstation software (version B.03.01).

3. Results and discussion

The following sections present and discuss the results obtained from UVA photolysis, adsorption onto the catalyst and photocatalytic OFX removal experiments.

3.1. OFX UVA direct photolysis

In a first series some experiments of OFX UVA photolysis (absence of TiO_2) were carried out. After 2 h of UVA radiation (black light) exposure the conversion of OFX 15 μM was low (<4%). The results were as expected taking into account the low overlap between the emission and the absorption spectra (see Fig. 1b) the low photon flux of the lamps used and the low quantum yield of OFX photolysis (1.5×10^{-3} to 3×10^{-3} mol einstein^{-1}, [13]). From Fig. 1b it is also deduced that the cationic species that predominates at pH < pKa_1 (pKa_1 = 6.2 and pKa_2 = 8.2, [14]), presents an

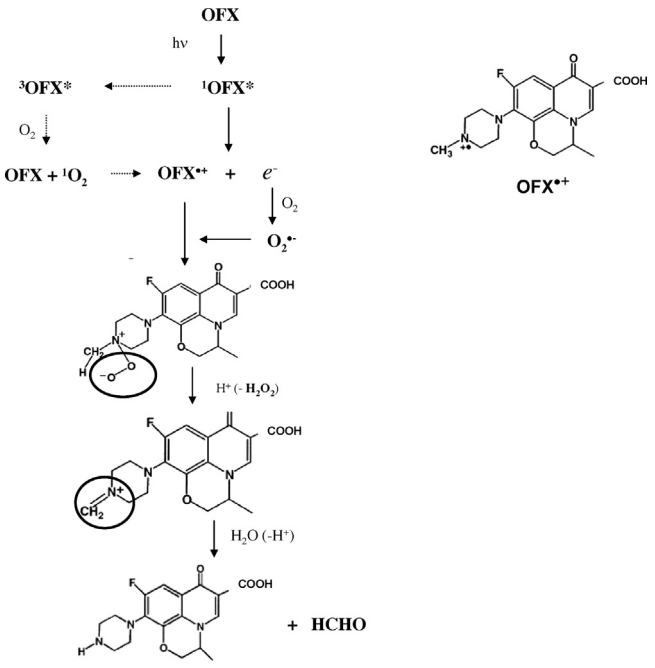

Fig. 2. Mechanism of OFX photodegradation. Adapted from [17].

absorptivity at the 350–400 nm wavelength range higher than the rest of OFX species (anionic, zwiterionic and neutral).

Despite of the low photodegradation of OFX attained (~5% after 2 h), the formation of hydrogen peroxide and formaldehyde from OFX photolysis under black light has been experimentally determined (not shown), and ~1 mole of each compound was formed per mol of OFX removed. This aspect was confirmed with experiments done using natural sunlight instead of black light. The results, available in the supporting information (see Fig. S2), indicate that the photolysis of OFX, faster under solar light due to a higher photon flux as well as the contribution of more energetic radiations, clearly leads to the formation of H_2O_2 and HCHO. From Fig. S2 the ratio between moles of HCHO formed per mole of OFX seems to be lower than one, which could be attributed to the photolysis of HCHO. This compound absorbs at $\lambda < 360$ nm and generates transient species that further evolve to the formation of hydroperoxide radical among other species [15].

Literature reports that OFX can absorb UVA radiation and generate singlet oxygen ($^1O_2$) through the following steps [16]:

$$OFX \xrightarrow{h\nu} {}^1OFX^* \rightarrow {}^3OFX^* \quad (1)$$

$${}^3OXF^* + O_2 \xrightarrow{k=2\times10^{10}\,M^{-1}\,s^{-1}} OFX + {}^1O_2 \quad (2)$$

where $^1OFX^*$ and $^3OFX^*$ are the singlet and triplet excited states of OFX, respectively. Navaratnam and Claridge [16] also reported the possible formation of the cationic radical $OFX^{\bullet+}$ and superoxide ion radical ($O_2^{\bullet-}$) through reaction (3):

$${}^3OFX^* + {}^1O_2 \rightarrow OFX^{\bullet+} + O_2^{\bullet-} \quad (3)$$

Similarly, Cuquerella et al. [17] proposed the mechanism shown in Fig. 2 where $^1OFX^*$ is formed from OFX photolysis under UV light. This single excited state can (i) photoionizate, with generation of $OFX^{\bullet+}$ and e^-, the later reacting with dissolved oxygen to give $O_2^{\bullet-}$ and (ii) in a minor extension, pass to a triplet state that further transfers energy to O_2 with generation of $^1O_2$. As for (i), the reaction between $^1O_2$ and OFX produces $OFX^{\bullet+}$ and $O_2^{\bullet-}$. The interaction between both radicals eventually leads to OFX demethylation with formation of 1 mole of hydrogen peroxide and 1 mole of formaldehyde per mole of OFX photodegraded.

The evolution of H_2O_2 and HCHO formed versus OFX eliminated showed in Fig. S2 clearly supports the mechanism described in Fig. 2 OFX acting as photosensitizing agent. In fact, the phototoxicity of this fluoroquinolone antibiotic has been reported to be related to the generation of different ROS [18,19].

3.2. OFX adsorption on TiO_2

In other series of experiments, the adsorption of OFX on the semiconductor TiO_2 in the dark was studied. According to the accepted scheme (reactions (4)–(8)), organic compounds adsorbed at the catalyst surface (TiO_2-EC) are more easily removed due to the participation of generated positive holes (h^+) and/or $HO^\bullet$ for their oxidation through reactions (5) and (8), although the formation of $HO^\bullet$ from adsorbed water (reaction (6)) seems not to be possible from a thermodynamic and kinetic point of view [20,21]:

$$TiO_2 \overset{h\nu}{\rightleftarrows} TiO_2(h^+, e^-) \quad (4)$$

$$h^+ + TiO_2\text{-EC} \overset{h\nu}{\rightleftarrows} TiO_2\text{-EC}^{\bullet+} \quad (5)$$

$$h^+ + TiO_2\text{-}H_2O \rightarrow TiO_2\text{-}HO^\bullet \quad (6)$$

$$h^+ + TiO_2\text{-OH} \rightarrow TiO_2\text{-}HO^\bullet \quad (7)$$

$$TiO_2\text{-EC} + TiO_2\text{-}HO^\bullet \rightarrow P \quad (8)$$

At the conditions applied in this work, hardly 5% OFX was adsorbed on the TiO_2 surface after 2 h of contact time (the adsorption equilibrium was reached in about 15 min).

3.3. OFX photocatalytic degradation: effect of the presence/absence of different scavengers

In addition to reactions (4)–(8) the classical mechanism of photocatalytic oxidation has the following steps [20]:

$$e^- + O_2 \xrightarrow{k=1.9\times10^{10}\,M^{-1}\,s^{-1}} O_2^{\bullet-} \quad (9)$$

$$HO_2^\bullet \overset{pK_a=4.8}{\rightleftarrows} H^+ + O_2^{\bullet-} \quad (10)$$

$$2HO_2^\bullet \,(\text{or } 2O_2^{\bullet-} + 2H^+) \rightarrow H_2O_2 + O_2 \quad (11)$$

$$HO_2^\bullet \,(\text{or } O_2^{\bullet-}) + H_2O_2 \rightarrow H_2O + O_2 + HO^\bullet \quad (12)$$

$$H_2O_2 + HO^\bullet \xrightarrow{k=2.7\times10^{7}\,M^{-1}\,s^{-1}} O_2^{\bullet-} + H^+ + H_2O \quad (13)$$

$$e^- + H_2O_2 \xrightarrow{k=1.1\times10^{10}\,M^{-1}\,s^{-1}} HO^\bullet + HO^- \quad (14)$$

$$EC + HO^\bullet \rightarrow P \quad (15)$$

where P are the reaction products.

According to this mechanism, depending on its concentration, hydrogen peroxide formed from reaction (11) can react with e^- through reaction (14) (competing with reaction (9)) and/or act as a sink of hydroxyl radicals through reaction (13). According to this mechanism, the generation of H_2O_2 is a key step for $HO^\bullet$ formation in the bulk water.

In this work, the photocatalytic degradation of 15 μM of OFX at pH 7 (perchloric/perchlorate 0.03 M) using 0.1 g L^{-1} of TiO_2 was first studied in aerated media and absence of other scavengers (control run). The control run was repeated every month and the evolution of OFX, H_2O_2, TAC and TOC was measured in order to check the reproducibility of results. In the case of HCHO the evolution of its concentration with time was analyzed during one of these runs.

Results of control run and error bars are shown in Fig. 3a. As for the photolytic experiments, the removal of the antibiotic by TiO_2/UVA goes hand in hand with the formation of both H_2O_2

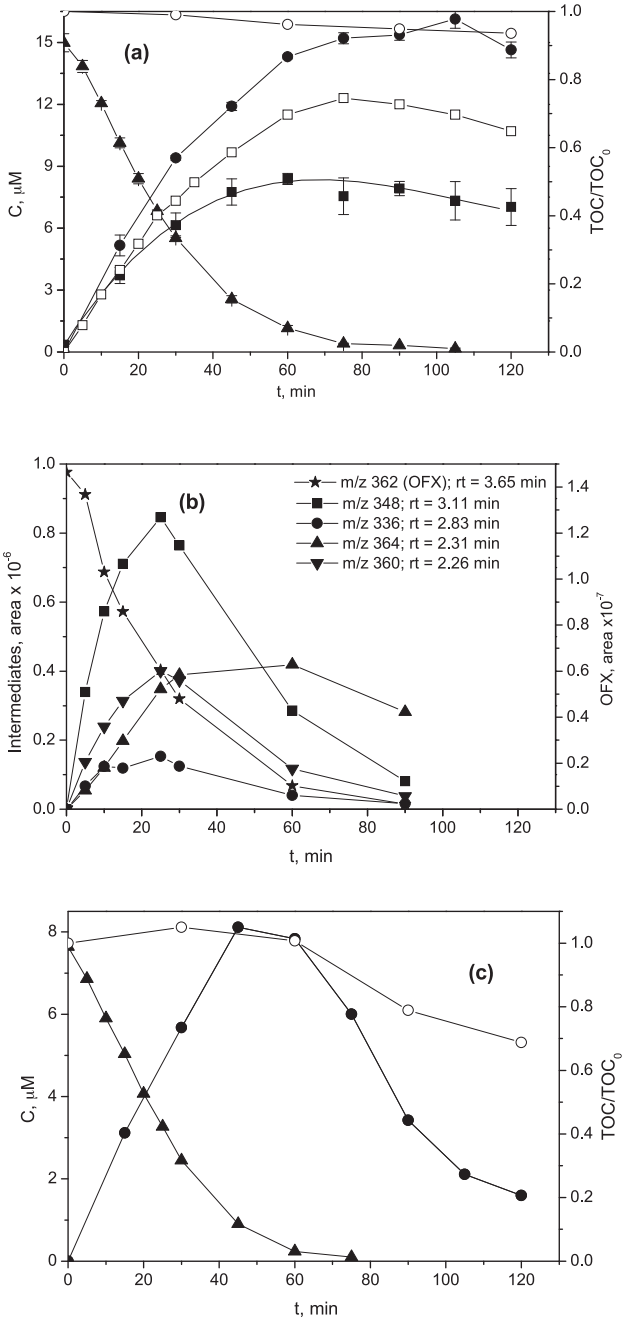

Fig. 3. Evolution of the different compounds and parameters analyzed with time. (a and b) control runs ($[OFX]_0 = 15\ \mu M$); (c) $[OFX]_0 = 7.5\ \mu M$. Symbols for (a and c) (▲) OFX; (●) H_2O_2; (■) TAC-I; (□) HCHO, and (○) TOC. Experimental conditions: $[TiO_2] = 0.1\ g\ L^{-1}$; pH 7 (0.03 M $HClO_4/ClO_4^-$); $V_T = 3\ L$; $I_0 = 7.33 \times 10^{-7}$ Einstein s^{-1}; 20–23 °C; air bubbling.

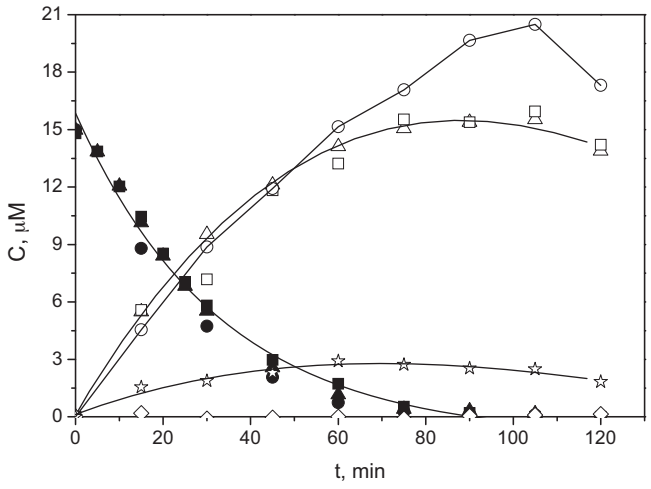

Fig. 4. Changes of OFX (solid symbols) and H_2O_2 (open symbols) concentrations during the photocatalytic elimination of OFX. Influence of t-BuOH. Symbols: (▲, △) $[OFX]_0 = 15\ \mu M$ (control run); (■, □) $[OFX]_0 = 15\ \mu M$, $[t\text{-BuOH}]_0 = 0.01$ M; (●, ○) $[OFX]_0 = 15\ \mu M$, $[t\text{-BuOH}]_0 = 0.1$ M; (☆) $[t\text{-BuOH}]_0 = 0.1$ M (absence of OFX); (◊) absence of any organic. Experimental conditions: $[OFX]_0 = 15\ \mu M$; $[TiO_2] = 0.1\ g\ L^{-1}$; pH 7 (0.03 M $HClO_4/ClO_4^-$); $V_T = 3\ L$; $I_0 = 7.33 \times 10^{-7}$ Einstein s^{-1}; 20–23 °C; air bubbling.

and HCHO (during the first 30 min, 1 mole of H_2O_2 and ~1 mole of HCHO are formed per mole of OFX degraded). In other words, TiO_2 increases the reductive demethylation rate of OFX if compared to UVA irradiation only effect without altering the products of reaction. In Fig. 3a it is also seen that as long as there is OFX in solution hydrogen peroxide accumulates in the media and reach a maximum that coincides with the initial concentration value of OFX. This suggests that reactions (12)–(14) do not develop while OFX is present. The evolution of TAC-I (expressed as OFX equivalents) and TOC with time is also shown in Fig. 3a. As observed, the intermediates formed present half the antioxidant capacity of the parent compound and almost no mineralization was attained at the conditions applied in these runs. On the other hand, Fig. 3b shows the variation with time of the area of the different peaks identified by LC–ESI-MS from a control run experiment. The analysis indicates the formation of *m/z* 348, 336, 364 and 360 intermediates during the first steps of OFX (*m/z* 362) removal. As expected, according to previous works the compound with *m/z* 348 corresponds to demethylated OFX [22–24]. Intermediates with *m/z* 336.13 and *m/z* 360 have also been detected by other authors although the molecular structures proposed differ (see Fig. S3, supporting information).

As shown in Fig. 3c similar tendencies were observed regardless of the initial OFX concentration. Thus, when initial OFX concentration was lower (7.5 μM) the H_2O_2 formed also accumulates in the media until OFX has been completely removed. At this reaction time H_2O_2 starts to decrease until almost disappear which could be attributed to the development of reaction (12). In other words, the formation of $HO^\bullet$ in bulk water probably takes place only when there is no OFX. This would explain the results obtained in previous works when a mixture of different ECs was treated by TiO_2/UVA [4]. In addition, the time variation of H_2O_2 concentration during all the runs, as it is shown in Fig. 3, indicates that reaction (11) can not compete with the reaction between $OFX^{\bullet+}$ and $O_2^{\bullet-}$. In view of the above comments, although HO radical seems not to participate in OFX photocatalytic elimination it is probably the main species involved in the mineralization of the intermediates. Thus, in Fig. 3c a link between TOC removal (~30% after 2 h) and H_2O_2 elimination (probably due to reaction (12) with generation of $HO^\bullet$ radicals) is observed.

3.3.1. *Effect of the presence of hydroxyl radical scavengers: tert-butanol*

With the aim of clarifying any possible contribution of HO radicals in bulk water to the removal of OFX, some new OFX photocatalytic runs were carried out in the presence of the hydroxyl radical scavenger *t*-butanol (t-BuOH). The rate constant of the t-BuOH-HO reaction is $6.2 \times 10^8\ M^{-1}\ s^{-1}$ [25]. As shown in Fig. 4 the effect of t-BuOH (0.01 and 0.1 M) on the OFX photocatalytic oxidation was practically negligible corroborating the hypothesis that participation of HO radicals in OFX removal through reaction (15) is not important. Evolution of TAC-I with time was also found to be independent on the presence of t-BuOH (not shown).

As observed in Fig. 4, t-BuOH did not affect the formation rate of H_2O_2 during the first 60 min reaction in all cases. However, for further reaction times, the increase of t-BuOH concentrations leads to an increase of H_2O_2 concentration up to a maximum value at about 100 min. The difference between the maximum H_2O_2 concentrations obtained in absence and presence of 0.1 M t-BuOH was 4×10^{-6} M, close to that observed in the OFX-free photocatalytic oxidation run performed in the presence of 0.1 M t-BuOH (see also Fig. 4). Therefore, in the presence of a high concentration of t-BuOH (0.1 M) the increase of H_2O_2 concentration, once OFX has totally disappeared, can likely be related to the formation of HO radical and its participation in the alcohol oxidation with generation of H_2O_2 [26]. In summary, according to all these results, at pH 7 and 0.03 M perchloric/perchlorate aerated media, HO radical in bulk water are not formed nor involved on OFX photocatalytic removal. Under these conditions the reductive demethylation of the antibiotic takes place, with the formation of H_2O_2 and HCHO.

3.3.2. *Effect of the presence of electron donor species: 2-propanol, iodide and oxalate*

The possible participation of holes on OFX photocatalytic elimination has been checked in the presence of electron donors such as 2-propanol (2-PrOH), iodide (as potassium iodide, KI) and oxalate. These substances once adsorbed on the TiO_2 can act as electron donors and be oxidized by h^+ [27–31].

The influence of the presence of 0.1 M and 0.25 M 2-PrOH is shown in Fig. 5a. As it is the case of t-BuOH, 2-PrOH can act as $HO^\bullet$ radical scavenger (the rate constant of this reaction being 2×10^9 M^{-1} s^{-1} [25]). Besides, due to its lower size, 2-PrOH can be adsorbed on TiO_2 surface and act as an electron donor reacting with h^+ [32]. Hence, when using 2-PrOH as scavenger both aspects should be taken into account. As observed in Fig. 5a, contrary to t-BuOH, the effect of 2-PrOH on OFX removal rate was negative and increased with increasing the concentration of the alcohol. Since the participation of $HO^\bullet$ in bulk water in OFX removal has been ruled out, the negative effect of the presence of 2-PrOH must be related to its adsorption on TiO_2 and/or its reaction with h^+ avoiding/reducing the interaction between OFX and photoactive centers and therefore the formation of $OFX^{\bullet+}$ through this way. Regarding the evolution of H_2O_2 and TAC-I, the results (see Fig. S4, supporting information) indicate that whereas the presence of 2-PrOH had no effect on the TAC-I formed/OFX removed mol ratio (~0.5 in all cases), the presence of 0.1 M and 0.25 M 2-PrOH had a slight positive and clearly negative effect, respectively, on the amount of H_2O_2 formed per mole of OFX eliminated ratio.

The chemistry of I^- is even more complex than that of 2-PrOH. Iodide reacts with HO radicals to yield I_2 and eventually I_3^- ($kHO^\bullet = 7.7 \times 10^9$ M^{-1} s^{-1}, [33]). Once formed, both I_2 and I_3^- can react with $O_2^{\bullet-}$ and/or e^- to regenerate I^- [34]. The oxidation of I^- by the H_2O_2 formed [35], should also be considered since it could hinder the formation of $HO^\bullet$ through reaction (12). Moreover, I_3^-, if formed, could reduce the UVA absorption rate of the semiconductor since this species strongly absorb UVA radiation (maximum wavelength of absorption is 351 nm, with an extinction coefficient of 25,700 M^{-1} cm^{-1}, [36]).

Taking all the above in mind two new experiments were carried out by adding 3×10^{-4} M of KI in absence or presence of 0.1 M t-BuOH. The evolution of OFX during these runs is shown in Fig. 5b. As observed, the presence of KI leads to a decrease of the OFX removal rate compared to the KI-free experiment (control runs), more markedly when t-BuOH was also added.

Since HO radicals do not participate in OFX photocatalytic elimination, t-BuOH seems to prevent in some way the oxidation of the iodide present in bulk water to I_2/I_3^- thus allowing higher concentrations of I^- in solution. In this sense, the ratio between H_2O_2 formed and OFX removed (see Fig. S5 in supporting information) results to be quite similar for the control run and when both I^- and t-BuOH were added, whereas it was clearly lower in the presence of I^- and absence of the alcohol. These results could indicate that the oxidation of I^- by H_2O_2 is partially avoided when t-BuOH is present. The decomposition of 15 μM H_2O_2 in the presence of 3×10^{-4} M KI at pH 7 (0.03 M perchloric/perchlorate) has also been experimentally verified (not shown).

From the runs where I^- was used same conclusions are reached as for the case of 2-PrOH: at the conditions tested in this work h^+ participates on OFX photocatalytic oxidation. Nevertheless, the use of both compounds as electron donor is not very recommendable due to their reactivity toward different species as it has been previously discussed.

Oxalate has also been used as a hole scavenger by different authors [37–39]. Waldner et al. reported h^+ as responsible species of the black light TiO_2 (anatase) photocatalytic oxidation of this carboxylate [40]. While oxalate reacts relatively slowly with both HO radicals and hydrated electrons ($k = 1.5 \times 10^7$ M^{-1} s^{-1} and 3.5×10^7 M^{-1} s^{-1}, [41]), once adsorbed on TiO_2, it is oxidized by h^+ to CO_2 through the following reactions:

$$C_2O_4^{=} + h^+ \rightarrow C_2O_4^{-} \rightarrow CO_2 + CO_2^{\bullet-} \quad (16)$$

$$CO_2^{\bullet-} + O_2 \rightarrow CO_2 + O_2^{\bullet-} \quad (17)$$

As shown in Fig. 5c the presence of 10^{-3} M oxalate concentration exerts a negative effect on the elimination rate of OFX corroborating the participation of h^+ through reaction (5). Also, for comparison purposes the results obtained when 10^{-3} M oxalate, 0.25 M 2-PrOH or 3×10^{-4} M KI + 0.1 M t-BuOH was added are presented in Fig. 5d. It can be observed that during these three runs the conversion of OFX was practically the same indicating that at these conditions all h^+ are trapped.

Contrary to 2-PrOH and KI, the amount of H_2O_2 formed per mole of OFX removed when 10^{-3} M oxalate was added was practically the same as in the control run. In other words, oxalate does not alter the degradation pathway of OFX (a reductive demethylation with formation of HCHO and H_2O_2), nor react with the hydrogen peroxide formed. Moreover, at the conditions applied in this work, contribution of oxalate to H_2O_2 formation through the recombination of the $O_2^{\cdot-}$ formed from reaction (17) can be neglected. Therefore, among the electron donors investigated oxalate seems to be the most appropriate in order to check the contribution of h^+ to the photocatalytic oxidation of a given compound in water.

The results obtained corroborate the participation of h^+ in the photocatalytic removal of OFX. In the following section the participation of superoxide ion radical is investigated.

3.3.3. *Effect of the presence of superoxide ion radical anion scavengers:* p-*benzoquinone and tiron*

According to literature, *p*-benzoquinone (*p*-BQ) and tiron (sodium 1,2-dihydroxybenzene, 3-5-disulfonate) are very reactive toward $O_2^{\bullet-}$. The rate constant values of the reactions of $O_2^{\bullet-}$ with *p*-BQ and tiron are $0.9–1 \times 10^9$ M^{-1} s^{-1} [42,43] and 5×10^8 M^{-1} s^{-1} [44], respectively, the latter obtained by competition kinetics using *p*-BQ as competitor. *p*-Benzoquinone has already been used by several authors to check the involvement of superoxide ion radical on the photocatalytic degradation of different organics in water [39,45,46]. However, *p*-BQ has also a great capacity to trap electrons (the rate constant of this reaction is 1.35×10^9 M^{-1} s^{-1}, [47]) and to react with hydroxyl radicals (rate constant is 6.6×10^9 M^{-1} s^{-1}, [48]). Alegría et al. [49] reported that the *p*-BQ photoexcitation can lead to singlet oxygen whereas Garg et al. [50] have postulated that the quinones present in Natural Organic Matter (NOM) photolyse under sunlight giving rise to $O_2^{\cdot-}$ that further evolves to H_2O_2. Accordingly, the use of *p*-BQ as a scavenger of superoxide ion radical could not be appropriate. In

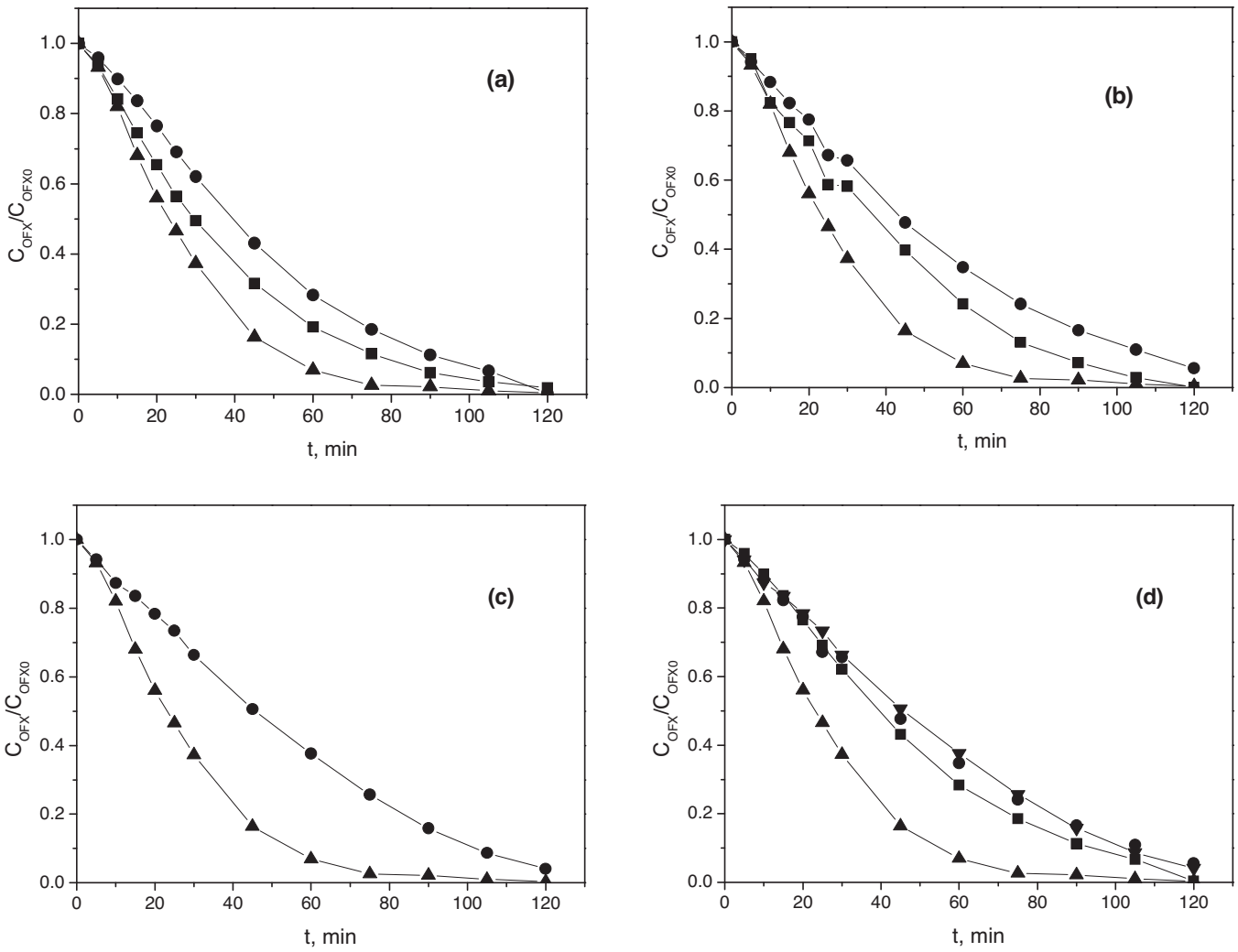

Fig. 5. Variation of normalized remaining concentration of OFX with time. Influence of different scavengers. (a) 2-PrOH. Symbols: (▲) control run; (■) $[2\text{-PrOH}]_0 = 0.1$ M; (●) $[2\text{-PrOH}]_0 = 0.25$ M. (b) KI. Symbols: (▲) control run; (■) $[KI]_0 = 3 \times 10^{-4}$ M; (●) $[KI]_0 = 3 \times 10^{-4}$ M and [t-BuOH] 0.1 M. (c) Oxalate. Symbols: (▲) control run; (●) [Oxalate] 10^{-3} M. (d) Comparison of scavengers. Symbols: (▲) control run; (■) $[2\text{-PrOH}]_0 = 0.25$ M; (●) $[KI]_0 = 3 \times 10^{-4}$ M and [t-BuOH] 0.1 M; (▼) [Oxalate] 10^{-3} M. Same experimental conditions as in Fig. 4.

Fig. 6a. the concentration changes of eliminated OFX and formed H_2O_2 with time using different concentrations of *p*-BQ (20 μM and 10^{-3} M) is shown. As observed, *p*-BQ seems to exert a negative effect on the elimination of the antibiotic which could suggest the participation of $O_2^{\cdot-}$ on the process. On the other hand, *p*-BQ and/or the semiquinone and/or hydroquinone formed highly promote the generation of H_2O_2 and/or interfere on Masschelein's method. In other words, the redox properties of *p*-BQ and its high reactivity toward different species make the use of *p*-BQ as $O_2^{\cdot-}$ scavenger not recommendable.

In view of these results new experiments were done in the presence of tiron. Tiron is commonly used to test the existence of $O_2^{\cdot-}$ within the cells (process that could be involved on aging and tumors; [51,52]). This compound could also react with hydroxyl radicals if formed (the rate constant is 10^9 M^{-1} s^{-1}; [53]) and its adsorption on TiO_2 is unknown. Accordingly, the influence of a 20 μM tiron concentration on the photocatalytic degradation of a 15 μM OFX solution was performed by adding 0.1 M t-BuOH as $HO^{\bullet}$ scavenger; or adding 0.25 M 2-PrOH as both $HO^{\bullet}$ and h^+ scavenger. The results obtained are shown in Fig. 6b. As observed, regardless of the alcohol used, tiron significantly inhibited the removal of OFX, indicating the important role of superoxide ion radical on the elimination of the antibiotic. Contrary to *p*-BQ there was no H_2O_2 generation at all during these runs. Although low or null amount of H_2O_2 was expected (the release of H_2O_2 needs the addition of $O_2^{\cdot-}$ to $OFX^{\bullet+}$, see Fig. 2), the results of Fig. 6b should be taken with caution since it has been experimentally verified that tiron interferes negatively on Masschelein's method. Thus, a 1:2 Co(II):tiron yellow complex is formed in alkaline conditions and also Co(II) catalyses the H_2O_2–tiron oxidation [54,55].

As in the case of the mechanism presented in Fig. 2 for the photolytic removal of OFX, the results obtained corroborates the participation of $O_2^{\bullet-}$ as one of the main species involved in the photocatalytic elimination of the antibiotic. The possible contribution of singlet oxygen to OFX removal is discussed in the following section.

3.3.4. *Effect of the presence of singlet oxygen scavengers: azide*

Literature reports photocatalytic degradation studies where sodium azide (NaN_3) has been used as singlet oxygen ($^1O_2$) quencher [56–59]. It should be noted that N_3^- is very reactive toward $^1O_2$ (rate constant of this reaction is 2×10^9 M^{-1} s^{-1}, [58]) with formation of azidyl radical ($N_3^{\bullet}$) and the superoxide radical ion, and its reactivity toward the hydroxyl radicals is even higher ($kHO^{\bullet} = 1 \times 10^{10}$ M^{-1} s^{-1}; [58]), also leading to $N_3^{\bullet}$ and the HO^- anion. The azide ion can also adsorb on the TiO_2 surface and act as

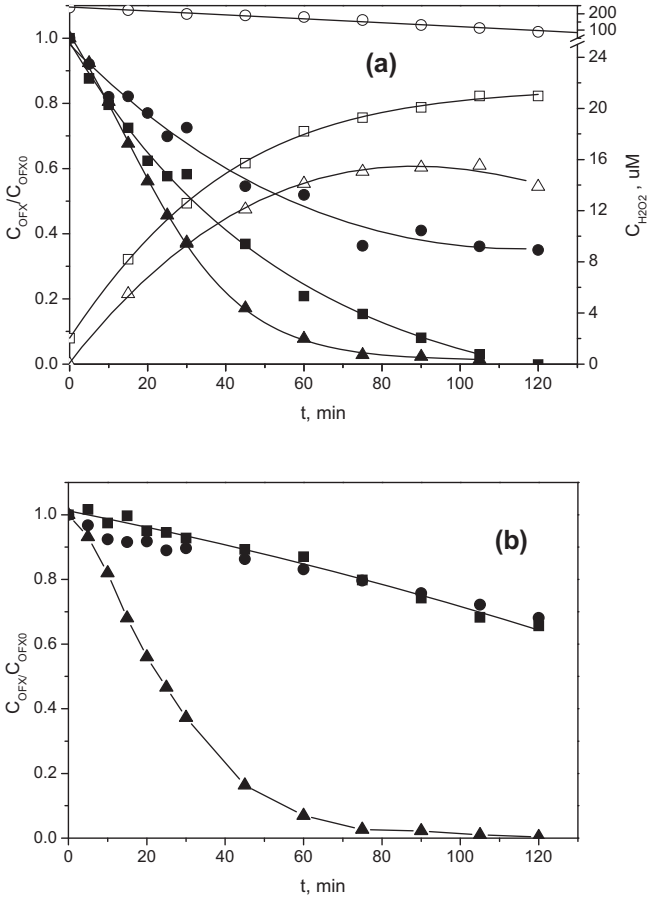

Fig. 6. Variation of OFX (solid symbols) and H_2O_2 (open symbols) concentrations with time. Influence of the presence of (a) *p*-benzoquinone. Symbols: (▲) control run; (■) $[p\text{-BQ}]_0 = 20\ \mu M$; (●) $[p\text{-BQ}]_0 = 10^{-3}$ M. (b) Tiron. Symbols (▲) control run; (■) $[\text{Tiron}]_0 = 20\ \mu M$; [t-BuOH] = 0.1 M; (●) $[\text{Tiron}]_0 = 20\ \mu M$; [2-PrOH] = 0.25 M. Same experimental conditions as in Fig. 4.

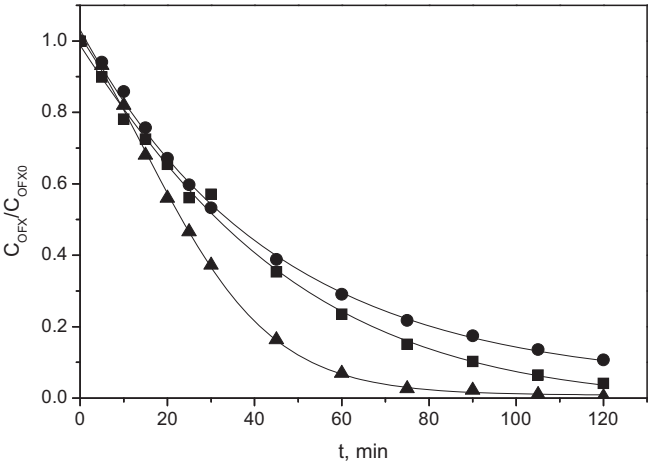

Fig. 7. Variation with time of normalized remaining concentration of OFX. Influence of the presence of azide. Symbols: (▲) control run; (■) $[NaN_3]_0 = 0.01$ M; (●) $[NaN_3]_0 = 0.01$ M, [2-PrOH] = 0.25 M. Same experimental conditions as in Fig. 4.

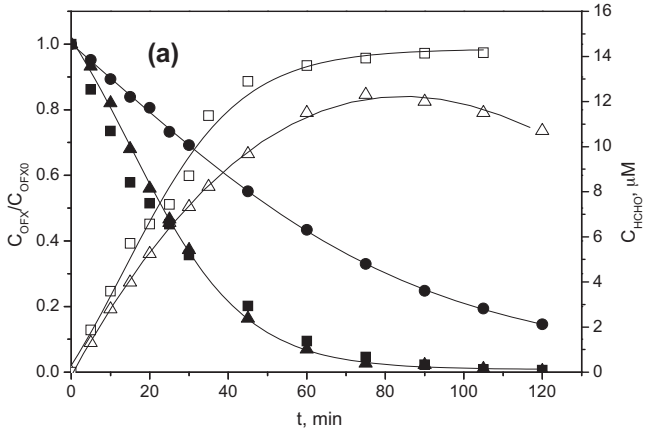

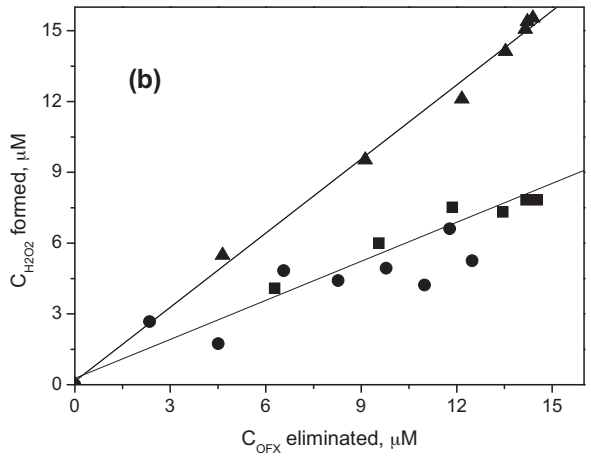

Fig. 8. Variation with time of (a) normalized remaining concentration of OFX (solid symbols) and concentration of formaldehyde formed (open symbols). (b) Relation between formed H_2O_2 and eliminated OFX. Influence of the presence of phosphate. Symbols: (▲) control run; (■) $[PO_4^{3-}]_0 = 0.01$ M; (●) $[PO_4^{3-}]_0 = 0.01$ M, [t-BuOH] = 0.1 M; Other experimental conditions as in Fig. 4.

electron donor by reacting with h^+ to yield $N_3^{\bullet}$. In other words, the possible negative effect NaN_3 on the photocatalytic degradation of a given compound in water could be attributed to the quenching of species different than $^1O_2$. In order to avoid the oxidation of azide ion by $HO^{\bullet}$ and/or h^+, photocatalytic degradation runs of OFX were carried out with 0.01 M NaN_3 in the absence and presence of 0.25 M 2-PrOH. Fig. 7 shows the results obtained. As it can be seen there is no difference of results during the first approximately 10 min of reaction comparing to control run. At higher reaction times, the presence of NaN_3 exerts a slight negative effect on OFX removal which is slightly increased when 2-PrOH is also present. These results suggest some participation of $^1O_2$ in OFX removal but they are not conclusive given the high reactivity of NaN_3 as commented before. On the other hand, in the experiments with NaN_3 formation of H_2O_2 was negligible regardless of the presence of 2-PrOH (see Fig. S6, supplementary info, where for comparison purposes the results obtained when 0.025 M 2-PrOH concentration added in the absence of NaN_3 have also been included). When 2-PrOH was present, the ratio between H_2O_2 formed and OFX degraded was higher in the absence of NaN_3. In this work it has been experimentally observed that NaN_3 does not decompose H_2O_2 nor interfere on the Masschelein's method. Then, when NaN_3 is present hydrogen peroxide formed is removed through some unknown competitive reaction in which the azidyl radical could participate.

The results obtained are similar to those of Stylidi et al. [56] when studying the visible light photocatalytic oxidation of acid orange 7 (AO7). As OFX, AO7 also acts as photosensitizer, so that the excited singlet state ($^1AO7^*$) can inject electrons to the TiO_2 conduction band to form the corresponding radical cation $AO7^{\bullet+}$. In absence of NaN_3 hydrogen peroxide was formed but in the presence of NaN_3, after an initial period, AO7 removal was slightly inhibited

Table 1
Scavengers used and their effect on TiO_2/UVA elimination of OFX at pH 7.[a]

Compound/concentration	Reactivity	Effects observed (compared to control runs)	It means that . . .	Comments
None (control runs)		1 mole of H_2O_2 and 1 mole of HCHO are formed per mole of OFX degraded	In these conditions: mainly reductive demethylation	
t-BuOH/0.01 and 0.1 M	Reacts with $HO^\bullet$ in bulk water	No effect	$HO^\bullet$ does not participate In these conditions: mainly reductive demethylation	t-BuOH is oxidized once OFX has been completely removed: $HO^\bullet$ is not formed in bulk water if OFX is present H_2O_2 is formed from t-BuOH-$HO^\bullet$ reaction
2-PrOH/0.1 and 0.25 M	Reacts with $HO^\bullet$ in bulk water Once adsorbed on TiO_2, reacts with $HO^\bullet/h^+$ at the catalyst surface	Their presence negatively affects the degradation rate of OFX The three reagents give rise to practically the same effects	$HO^\bullet$ at the catalyst surface (if formed) does not participate h^+ generated at the catalyst surface contributes to OFX degradation	Taking into account its adsorption on the catalyst surface and its electron donor capacity, 2-PrOH should not be used as $HO^\bullet$ scavenger
Iodide (I^-)/3×10^{-4} M (in absence/presence of t-BuOH 0.1 M)	Reacts with $HO^\bullet$ in bulk water Once adsorbed on TiO_2, reacts with $HO^\bullet/h^+$ at the catalyst surface			Oxidation of I^- gives I_2 (oxidant; photoactive). I^- reacts with H_2O_2 The use of I^- as h^+ scavenger is not recommended
Oxalate ($C_2O_4^{=}$)/10^{-3} M	Once adsorbed reacts with h^+			The reactivity of oxalate toward $HO^\bullet$ is relatively low. Good as h^+ scavenger
p-Benzoquinone/20 μM and 10^{-3} M	Reacts with $HO^\bullet$ in bulk water As an electron acceptor it can be reduced by both e^- and $O_2^{\bullet-}$	Negative effect on OFX degradation rate	Contribution of $O_2^{\bullet-}$ to OFX elimination	*p*-BQ and/or semiquinone/hydroquinone promote H_2O_2 generation and/or interfere positively on Masschelein's method The use of *p*-BQ as $O_2^{\bullet-}$ scavenger is not recommended
Tiron/20 μM (in absence/presence of t-BuOH)	Reacts with $HO^\bullet$ in bulk water Is oxidized to a semiquinone by $O_2^{\bullet-}$	Strong negative effect on OFX degradation rate	Important contribution of $O_2^{\bullet-}$ to OFX elimination	Tiron interferes (negatively) on the analysis of H_2O_2 by Masschelein's method
Azide (N_3^-)/0.01 M (in absence/presence of 2-PrOH 0.25 M)	Reacts with singlet oxygen ($^1O_2$) Reacts with $HO^\bullet$ in bulk water Once adsorbed, reacts with $HO^\bullet/h^+$ at the catalyst surface	Slight negative effect on OFX degradation rate H_2O_2 has not been detected: If formed, H_2O_2 quickly decompose	It is not possible to stablish the generation/participation of singlet oxygen due to the high reactivity of N_3^- toward different species	Its adsorption onto the catalyst probably inhibits the interaction OFX-TiO_2 surface
PO_4^{3-}/0.01 M (in absence/presence of t-BuOH)[b]	Once adsorbed on TiO_2 promotes the generation of $HO^\bullet$ in bulk water	No effect on OFX degradation nor formaldehyde formation rates Strong negative effect on H_2O_2 generation	$HO^\bullet$ formed in bulk water leads to the oxidative demethylation of OFX	PO_4^{3-} adsorbed on TiO_2 inhibits the interaction OFX-TiO_2.

[a] 15 μM OFX in 0.03 M perchloric/perchlorate aerated media.
[b] Without perchloric/perchlorate.

and H_2O_2 was not formed. In summary, due to the high reactivity of azide toward different oxidant species as well as the unknown reactivity of the azidyl radical, it is not possible to establish the participation of $^1O_2$ on the photocatalytic removal of OFX. In any case, its contribution would be irrelevant.

3.3.5. *Effect of the presence of oxygen as an electron acceptor*

As it is known oxygen can act as an electron acceptor avoiding the recombination of electrons and holes and contributing to the formation of different ROS through reaction (9). Taking this in mind, the influence of O_2 was studied by continuously bubbling air (control run) or nitrogen or without feeding any gas to an air-saturated aqueous OFX solution. The OFX removal rate was very similar in all cases (not shown) and the absence of O_2 (bubbling N_2) had only a very small negative effect at long contact times (more than 60 min). Therefore, the existence of dissolved oxygen does not seem to be crucial for the elimination of the antibiotic. An et al. [60] proposed that fluoroquinolones react with the solvated electrons of the TiO_2 surface, the rate constant of the OFX–e^- reaction being $2 \times 10^{10}\ M^{-1}\ s^{-1}$ [16]. Thus, the little importance of O_2 on OFX degradation rate suggests that in absence of O_2 the antibiotic could also be degraded through its reaction with electrons. On the other hand, the ratio between H_2O_2 formed and OFX eliminated was practically the same when oxygen was initially present or bubbled, whereas H_2O_2 was not formed when nitrogen was bubbled. This could indicate that: (a) in absence of O_2 electrons reacts also with the H_2O_2 formed (reaction (13)) and/or (b) in absence of O_2 the degradation mechanism of OFX changes. In an attempt to clarify this aspect the evolution of the absorbance at 260 nm with time was followed. The results (see Fig. S7, supporting info) indicate that the time profile of $A_{260\,nm}$ was practically the same when some oxygen (low or in excess) was present in water, the absorbance continuously decreasing with reaction time. However, in absence of O_2 (N_2 bubbling), the $A_{260\,nm}$ value kept constant and only started to decrease once OFX was totally removed (after 60 min reaction). Then, it seems that in absence of oxygen the photocatalytic elimination of OFX is possible but follows a pathway different from that shown in Fig. 2.

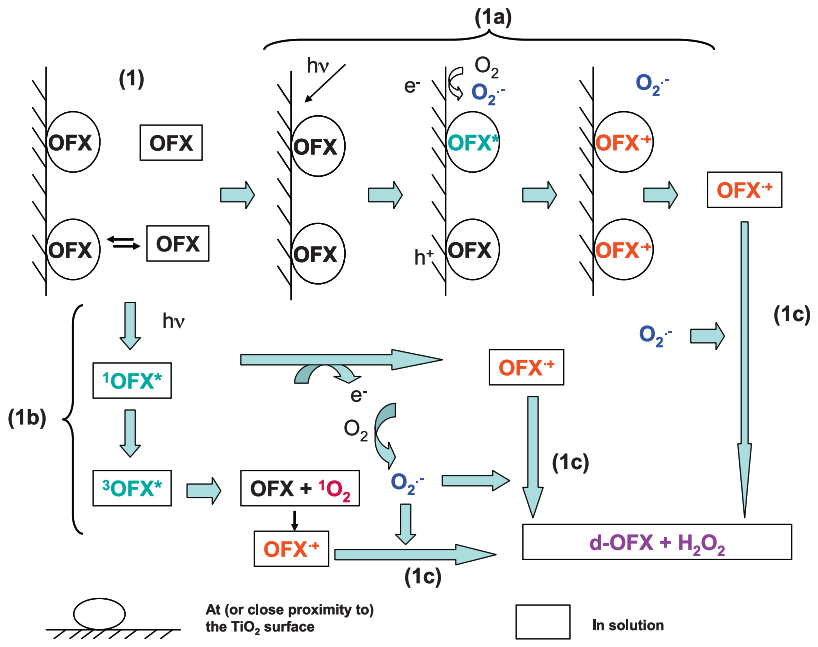

Fig. 9. Mechanism proposed for the TiO_2/UVA degradation of OFX at pH 7 in perchloric/perchlorate aerated medium.

3.3.6. Effect of the presence of phosphate

The results obtained in this work differ significantly from those reported by van Doorslaer et al. [61]. With the use of scavengers (iodide for h^+ and 2-PrOh for HO•) the authors concluded that the main species involved on the first-step TiO_2 P25/black light elimination of the fluoroquinolone moxiofloxacin (MOFX) at pH 7 were h^+ (64%) and HO• (24%). Although the advantages and disadvantages of the use of both substances as scavengers have been discussed in previous sections, the results clearly differ from those obtained in this work. Comparing both studies, the main difference with van Doorslaer's experimental conditions, apart from the use of a different fluoroquinolone, was the presence of 0.01 M phosphate buffer. As a consequence new runs were performed using 0.01 M phosphate buffer instead of 0.03 M perchloric/perchlorate. As shown in Fig. 8a phosphate exerts no effect on OFX degradation nor on HCHO formation rates (the latter during the first 30 min; for longer treatment times the concentration of HCHO in solution was lower in absence of phosphate), but its presence drastically reduces the formation of H_2O_2 as shown in Fig. 8b. On the other hand, the evolution of $A_{260\,nm}$ when PO_4^{3-} was added differed from that of the control run, similarly to what was observed in absence of O_2 (see Fig. S7). The different behavior of both H_2O_2 and $A_{260\,nm}$ suggests a change in the mechanism of OFX removal when phosphate is present.

Zhao et al. [62] found that TiO_2 surface-bound phosphate anion can affect both the rate and pathway of photocatalytic reactions. Thus, the authors propose that for substrates that are weakly adsorbed on TiO_2 (as it is the case of OFX) the degradation is accelerated in the presence of phosphate due to a higher production of HO• radicals. On the contrary, the degradation rate decreases for substrates with strong adsorption on TiO_2 since, according to Zhao et al., PO_4^{3-} hinders the direct hole oxidation pathway. The enhancement of HO• production by phosphate has also been observed by other authors [63]. In view of the above, to check if the formation and participation of HO• in OFX removal is promoted by phosphate anion a new experiment was performed adding 0.01 M PO_4^{3-} and 0.1 M t-BuOH to the reaction media. As deduced from Fig. 8a the addition of the alcohol had a strong negative effect and the elimination rate of OFX was halved. It proves that PO_4^{3-} not only promotes the generation of HO• radicals and their participation in OFX oxidation (oxidative demethylation without H_2O_2 formation) but also impedes the development of those reactions that need the interaction between OFX and the catalyst surface. Moreover, the higher concentration of HCHO observed at $t > 30$ min when phosphate was used could indicate that the adsorption of formaldehyde and its interaction with the catalyst surface is also avoided.

Finally, the effect of the different scavengers/promoters studied and some important points about their use are summarized in Table 1.

3.4. Possible mechanism of OFX photocatalysis

From the results presented and discussed in the above sections the mechanism showed in Fig. 9, similar to that of Cuquerella et al. [17] (see Fig. 2), is proposed for the photocatalytic elimination of OFX in perchloric/perchlorate aerated medium at pH 7.

In a first step OFX has to approach the surface of the catalyst (adsorption seems not to be required but close proximity). Via 1a consists of UVA absorption and TiO_2 excitation to yield the h^+–e^- couple and also OFX* excited stated. Once formed OFX* would transfer an electron to the TiO_2 conduction band generating OFX•+, a very common mechanism for photosensitizers [56,64–66]. Adsorbed OFX (and/or very closed OFX molecules) could also react with h^+ to yield the OFX•+ radical whereas dissolved oxygen would react with e^- to form the superoxide ion radical. In a minor extension due to the type of light use (black light), through via 1b OFX molecules in solution could be excited to their singlet (^{1}OFX*) and, even, triplet (^{3}OFX*) states to give rise to the OFX•+ radical as proposed by Cuquerella et al. Finally, through via 1c the radical cation OFX•+ would react with the superoxide ion radical to eventually demethylated OFX (d-OFX) with formation of H_2O_2 and formaldehyde. According to this mechanism a stoichiometric ratio of 1 mol of H_2O_2 and 1 mol of HCHO formed per mol of OFX removed is expected, in agreement with the experimental results.

4. Conclusions

Superoxide ion radical and positive holes are the main species involved in the photocatalytic degradation of OFX in

perchloric/perchlorate aerated medium at pH 7. At these conditions the reductive demethylation of the antibiotic takes place with generation of formaldehyde and hydrogen peroxide. In absence of oxygen the degradation rate of OFX is practically the same but the elimination pathway differs. Phosphate anion, if present, adsorbs on TiO_2 promoting the formation of bulk $HO^{\bullet}$ and, thus, the oxidative demethylation of OFX, lowering the yield of H_2O_2 formation. In summary, OFX can be photocatalytically reduced or oxidized (with or without generation of H_2O_2, respectively) depending on the experimental conditions.

On the other hand, according to OFX removal results, for studies of photocatalytic degradation of organics in water the use of t-BuOH, oxalate and tiron seems to be recommendable to confirm or not the participation of $HO^{\bullet}$ in bulk solution, h^+ and $O_2^{\bullet -}$, respectively. Hence, for a practical case, once main species involved in the removal of a given compound are known, it would be possible to establish the optimized experimental conditions to improve the conversion rates by favoring the formation of such species.

Acknowledgements

Authors thank the Spanish MINECO and European Feder Funds (CTQ2012-35789-C02-01) and Junta de Extremadura (Project GRU10012) for the economic support.

Appendix A. Supplementary data

Supplementary data associated with this article can be found, in the online version, at http://dx.doi.org/10.1016/j.apcatb.2014.11.002.

References

[1] J.Q. Jiang, Z. Zhou, V.K. Sharma, Microchem. J. 110 (2013) 292–300.
[2] S. Malato, P. Fernández-Ibáñez, M.I. Maldonado, J. Blanco, J.W. Gernjak, Catal. Today 147 (2009) 1–59.
[3] L. Prieto-Rodríguez, S. Miralles-Cuevas, I. Oller, P. Fernández-Ibáñez, A. Agüera, J. Blanco, S. Malato, Appl. Catal. B: Environ. 128 (2012) 119–125.
[4] E.M. Rodríguez, G. Márquez, E.A. León, P.M. Álvarez, A. Amat, F.J. Beltrán, J. Environ. Manage. 127 (2013) 114–124.
[5] B. Ohtani, O.O. Prieto-Mahaney, D. Li, R. Abe, J. Photochem. Photobiol. A 216 (2010) 179–182.
[6] Evonik-Degussa, 2008, NT-08-0032, http://epa.gov/oppt/nano/submissions.htm
[7] C.G. Hatchard, C.A. Parker, Proc. R. Soc. Lond. Ser. A 235 (1956) 518–536.
[8] W. Masschelein, M. Denis, R. Ledent, Water Sewage Works (1977) 69–72.
[9] R. Flyunt, A. Leitzke, G. Mark, E. Mvula, E. Reisz, R. Schick, C. von Sonntag, J. Phys. Chem. B 107 (2003) 7242–7253.
[10] V.L. Singleton, J.A. Rossi, Am. J. Enol. Viticult. 16 (1965) 144–158.
[11] K.I. Berker, F.A.O. Olgun, D. Ozyurt, B. Demirata, R. Apak, J. Agric. Food Chem. 61 (2013) 4783–4791.
[12] F. Belal, A.A. Al-Majed, A.M. Al-Obaid, Talanta 50 (1999) 765–786.
[13] K.H. Wammer, A.R. Korte, R.A. Lundeen, J.E. Sundberg, K. McNeill, W.A. Arnold, Water Res. 47 (2013) 439–448.
[14] H.A. Okeri, I.M. Arkewoh, Afr. J. Biotechnol. 7 (2008) 670–680.
[15] A. Gratien, B. Picquet-Varrault, J. Orphal, E. Perraudin, J.F. Doussin, J.M. Flaud, J. Geophys. Res. 112 (2007) 1–10.
[16] S. Navaratnam, J. Claridge. Photochem. Photobiol. 72 (2000) 283–290.
[17] M.C. Cuquerella, F. Boscá, M.A. Miranda, A. Belvedere, A. Catalfo, G. de Guidi, Chem. Res. Toxicol. 16 (2003) 562–570.
[18] N. Umezawa, K. Arakane, A. Ryu, S. Mashiko, M. Hirobe, T. Nagano, Arch. Biochem. Biophys. 342 (1997) 275–281.
[19] R.S. Ray, N. Agrawal, R.B. Misra, M. Farooq, R.K. Hans, Drug Chem. Toxicol. 29 (2006) 25–38.
[20] C.S. Turchi, D.F. Ollis, J. Catal. 122 (1990) 178–192.
[21] P. Salvador, J. Phys. Chem. C 111 (2007) 17038–17043.
[22] P. Calza, C. Medana, F. carbone, V. Giancotti, C. Baiocchi, Rapid. Commun. Mass Spectrom. 22 (2008) 1533–1552.
[23] E.M. Van Wieren, M.D. Seymour, J.W. Peterson, Sci. Total Environ. 441 (2012) 1–9.
[24] M.I. Vasquez, E. Hapeshi, D. Fatta-Kassinos, K. Kümmerer, Environ. Sci. Pollut. Res. 20 (2013) 1302–1309.
[25] M.S. Alam, B.S.M. Rao, E. Janata, Radiat. Phys. Chem. 67 (2003) 723–728.
[26] M.M. Schuchmann, C. von Sonntag, J. Phys. Chem.-US 83 (1979) 780–784.
[27] N. Serpone, I. Texier, A.V. Emeline, P. Pichat, H. Hidaka, J. Zhao, J. Photochem. Photobiol. A 136 (2000) 145–155.
[28] Y. Chen, S. Yang, K. Wang, L. Lou, J. Photochem. Photobiol. A 172 (2005) 47–54.
[29] F.J. Beltrán, A. Aguinaco, J.F. García-Araya, Water Res. 43 (2009) 1359–1369.
[30] G. Li, S. Ciston, Z.V. Saponjic, L. Chen, N.M. Dimitrijevic, T. Rajh, K.A. Gray, J. Catal. 253 (2008) 105–110.
[31] L.S. Zhang, K.H. Wong, D.Q. Zhang, C. Hu, J.C. Yu, C.Y. Chan, P.K. Wong, Environ. Sci. Technol. 43 (2009) 7883–7888.
[32] I. Carrizosa, G. Munuera, J. Catal. 49 (1977) 174–188.
[33] F. Taghipour, G.J. Evans, Radiat. Phys. Chem. 64 (2002) 203–213.
[34] G.V. Buxton, C.L. Greenstock, W.P. Helman, A.B. Ross, J. Phys. Chem. Ref. Data 14 (1988) 513–886.
[35] A.R. Conklin, A. Kessinger, J. Chem. Educ. 73 (1996) 838.
[36] Y. Bichsel, U. von Gunten, Anal. Chem. 71 (1999) 34–38.
[37] S.H. Yoon, J.H. Lee, Environ. Sci. Technol. 39 (2005) 9695–9701.
[38] W. Wang, L. Zhang, T. An, G. Li, H.Y. Yip, P.K. Wong, Appl. Catal. B: Environ. 108–109 (2013) 108–116.
[39] M.Q. Yang, Y. Zhang, N. Zhang, Z.R. Tang, Y.J. Xu, Sci. Rep. (2013), http://dx.doi.org/10.1038/srep03314 (available through www.nature.com/scientificreports).
[40] G. Waldner, R. Gómez, M. Neumann-Spallart, Electrochim. Acta 52 (2007) 2634–2639.
[41] B.G. Ershov, E. Janata, M.S. Alam, A.V. Gordeev, High Energ. Chem. 42 (2008) 1–6.
[42] P.S. Rao, E. Hayon, J. Phys. Chem. 79 (1975) 397–402.
[43] B.H.J. Bielski, D.E. Cabelli, R.L. Arudi, A.B. Ross, J. Phys. Chem. Ref. Data 14 (1985) 1041–1100.
[44] C.L. Greenstock, R.W. Miller, Biochim. Biophys. Acta 396 (1975) 11–16.
[45] S. Xu, J. Shen, S. Chen, M. Zhang, T. Shen, J. Photochem. Photobiol. B 67 (2002) 64–70.
[46] R. Palominos, J. Freer, M.A. Mondaca, H.D. Mansilla, J. Photochem. Photobiol. A 193 (2008) 139–145.
[47] M. Anbar, P. Neta, Int. J. Appl. Radiat. Isotopes 18 (1967) 493–523.
[48] M.N. Schuchmann, E. Bothe, J. von Sonntag, C. von Sonntag, J. Chem. Soc. Perkin Trans. 2 (1998) 791–796.
[49] A.E. Alegría, A. Ferrer, G. Santiago, E. Sepúlveda, W. Flores, J. Photochem. Photobiol. A 127 (1999) 57–65.
[50] S. Garg, A.L. Rose, T.D. Waite, Photochem. Photobiol. 83 (2007) 904–913.
[51] M. Sawada, J.C. Carlson, Mech. Ageing Dev. 41 (1987) 125–137.
[52] J.Y. Hwang, J. Lubow, D. Chu, H. Agadjanian, J. Sims, H.B. Gray, Z. Gross, D.L. Farkas, L.K. Medina-Kauwe, Mol. Pharm. 8 (2011) 2233–2243.
[53] W. Bors, M. Saran, C. Michel, Biochim. Biophys. Acta 582 (1979) 537–542.
[54] C.K. Bhaskare, S.K. Deshmukh, Z. Anal, Chemistry 277 (1975) 127.
[55] K. Isshiki, E. Nakayama, Talanta 34 (1987) 277–281.
[56] M. Stylidi, D.I. Kondarides, X.E. Verykios, Appl. Catal. B: Environ. 47 (2004) 189–201.
[57] C. Kanurakaram, S. Senthilvelan, S. Karuthapandian, J. Photochem. Photobiol. A 172 (2005) 207–213.
[58] Z. Xu, C. Jing, F. Li, X. Meng, Environ. Sci. Technol. 42 (2008) 2349–2354.
[59] Y.F. Rao, W. Chu, Environ. Sci. Technol. 43 (2009) 6183–6189.
[60] T. An, H. Yang, W. Song, G. Li, H. Luo, W.J. Cooper, J. Phys. Chem. A 114 (2010) 2569–2575.
[61] X. van Doorslaer, P.M. Heyndercks, K. Demeestere, K. Debevere, H. Van Langenhove, J. Dewulf. Appl. Catal. B: Environ. 111 (2012) 150–156.
[62] D. Zhao, C. Chen, Y. Wang, H. Ji, W. Ma, L. Zang, J. Zhao, J. Phys. Chem.-US (2008) 5993–6001.
[63] H. Liao, T. Reitberger, Catalysts 3 (2013) 418–443.
[64] Z.X. Zhou, S.P. Qian, S.D. Yao, Z.Y. Zhang, Dyes Pigments 51 (2001) 137–144.
[65] W.S. Kuo, P.H. Ho, Dyes Pigments 71 (2006) 212–217.
[66] A. Kathiravan, M. Chandramohan, R. Renganathan, S. Sekar, Spectrochim. Acta A 71 (2009) 1783–1787.